International Journal of Automotive Technology, Vol. 5, No. 4, pp. 303–309 (2004)

1229-9138/2004/018-09

DETECTION OF INTERFACIAL CRACK LENGTH BY USING ULTRASONIC ATTENUATION COEFFICIENTS ON ADHESIVELY BONDED JOINTS

N.-Y. CHUNG[1)*] and S.-I. PARK[2)]

[1)]Department of Mechanical Engineering, Soongsil University, Seoul 156-743, Korea
[2)]Department of Mechanical Engineering, Graduate School, Soongsil University, Seoul 156-743, Korea

(Received 30 August 2003; Revised 5 March 2004)

ABSTRACT–In this paper, an interfacial crack length has been detected by using the ultrasonic attenuation coefficient on the adhesively bonded double-cantilever beam (DCB) joints. The correlations between energy release rates which were investigated by experimental measurement, the boundary element method (BEM) and Ripling's equation are compared with each other. The experimental results show that the interfacial crack length for the ultrasonic attenuation coefficient and energy release rate increases proportionally. From the experimental results, we propose a method to detect the interfacial crack length by using the ultrasonic attenuation coefficient and discuss it.

KEY WORDS : Acoustic impedance, Adhesively bonded joint, Attenuation coefficient, Boundary element method, Compliance, Double-cantilever beam, Energy release rate, Interface crack, Transmission coefficient, Ultrasonic test

1. INTRODUCTION

Applications of adhesively bonded structures are increasing considerably as a result of the advance of adhesion technology, and the development of non-welding polymer materials and light-weight products with increased reliability and design efficiency, as well as the improvement of resistance to corrosion. Recently, adhesively bonded structures have been used in various engineering fields such as automobiles, rolling stocks, ships, IC package, aircraft, semiconductors, and medical instruments.

Especially, in the automobile industry, the joints of car bodies are gradually becoming dependent on adhesion for the purpose of reducing weight, and improving durability and safety. However, interfaces on the adhesively bonded joints are complex in the microscopic structures and interface crack is likely to occur owing to the conspicuous stress concentration on the interface edges. The initiation and propagation of an interface crack on the adhesively bonded joints of a car body leads to car accidents involving causalities and economic loss. To prevent damage caused by interface cracks, it is very important to detect the cracks on the interfaces of adhesively bonded joints in advance. Although applications of non-destructive tests on the homogeneous material have made substantial progress over the years, research for the detection of interface cracks on adhesively bonded joints has lagged behind. In addition, a standard for testing and evaluating methods has not been established in the non-destructive tests (Chung, 2001; 2002). Thus, providing a method to detect an interface crack is important in ensuring the safety and reliability of adhesively bonded joints (Kline, 1986; Derouiche, 1996; Song, 1998; Biwa, 2003; Xu, 1997).

One of non-destructive tests, the ultrasonic test, requires the consideration of frequency, density and the difference in acoustic impedance depending on the ultrasonic velocity which is applied to the detection of an interface crack on the adhesively bonded joints. As a crack propagates along an adhesive interface, the ultrasonic wave disperses, the sound pressure decreases, and the attenuation coefficient fluctuates (Si-Chaib, 2000; Pecorari, 2000; Castings, 2001).

Several researchers published their work on measurements of the dispersion and ultrasonic attenuation according to the crystal grain size of materials, as well as the change of materials using the immersion test. Kline investigated the dispersion and ultrasonic attenuation by using an ultrasonic spectrum (Kline, 1983). Ping measured the dispersion and ultrasonic attenuation of a material by the acoustic reflection and transmission pulse (Ping, 2001). However, the work done to detect an interface crack on adhesively bonded joints by ultrasonic tests has not been

*Corresponding author. e-mail: nychung@hanmail.net

published yet.

In this paper, therefore, the energy required for interfacial crack growth must be delivered and released as elastic energy and it then causes the ultrasonic attenuation as it propagates. The objective of this paper is to propose a method for detecting the interfacial crack length by using the ultrasonic attenuation coefficient.

The specimens of adhesively bonded DCB (double-cantilever beam) joints were provided with the aluminum alloy and cemedine 1500 adhesive. We derived the coefficient equation of the sound pressure transmission on the adhesively bonded joints with 4-layers and determined the factors affecting the derived equation.

Relations between the interfacial crack lengths and energy release rates, which are calculated by the compliance measurements, Ripling's equation (Ripling, 1964) and the boundary element method (BEM), are compared with each other. In order to investigate the detecting method of the interfacial crack length by using the ultrasonic attenuation coefficient, we compared the results and discussed the ratio of ultrasonic echo with the variation of the crack length, energy release rate, and ultrasonic attenuation coefficient.

2. EXPERIMENTAL

2.1. Shape and Dimensions of Specimen

In order to detect an interfacial crack length by using the ultrasonic attenuation coefficient, we produced the adhesively bonded DCB joints of the shape and dimensions shown in Figure 1. The length of the initial crack, a=10 mm, the length of adhesive joint, L=135 mm, and the thickness of adhesive layer, h_1=0.2 mm. The adherend is made of an aluminum alloy which is an opaque material, and the adhesive is a cemedine (Ced.) 1500 which is widely used as a structural adhesive. The

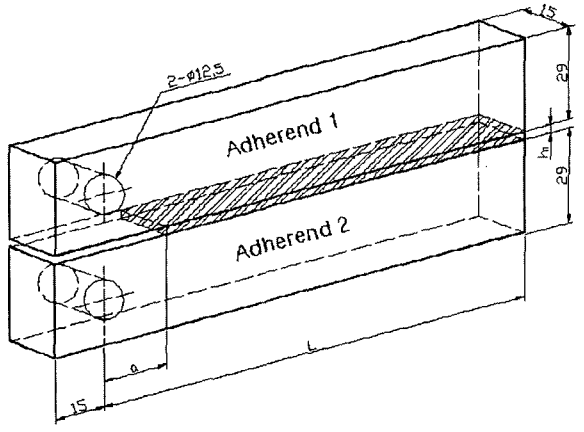

Figure 1. Shape and dimensions of an adhesively bonded DCB specimen.

Table 1. Material properties of DCB specimen.

Specimen materials	Material properties	Impedance, Z (10^6 kg/m^{2}s)	Longitudinal wave, V_L (m/s) / Shear wave, V_S (m/s)
Adherend	Aluminum	16.9	6,260 / 3,080
Adhesive	Ced. 1500	2.2	2,034 / 831
Couplant	Glycerin	2.4	1,880

Table 2. Ultrasonic properties of DCB specimen.

Specimen materials	Material properties	Density ρ (10^3 kg/m^3)	Young's modulus E (GPa)	Poisson's ratio ν
Adherend	Aluminum	2.70	65.56	0.32
Adhesive	Ced.1500	1.07	2.06	0.40

material and ultrasonic properties of the specimen are listed in Tables 1 and 2.

2.2. Manufacture of Specimen

After the plate of aluminum alloy was worked with a milling machine, the bonding area was polished roughly and then finely with #80 and #220 sandpaper, respectively. The bonding area was then washed with acetone, cleaned with water and dried. The adhesive of cemedine (Ced.) 1500 consisted of a main ingredient and hardener. Two beakers were filled with the main ingredient and hardener for a mixture ratio of 1 to 1 based on weight. The adhesive was stirred carefully to prevent the formation of voids, bubbles and impurities before it was applied to the surface of the adherend.

2.3. Experimental Method

The universal testing machine (Hounsfield H10KT) was used in the static tests and the load speed was kept at 0.5 mm/min under displacement control conditions. The displacement diagram of load-load point versus the interfacial crack length was recorded with an X-Y recorder. The displacement of load point was measured with a clip gauge. The compliance was calculated from the displacement diagram of load-load point obtained through the test and the energy release rate was calculated from the compliances. We measured the ultrasonic echo height and obtained the ultrasonic attenuation coefficient according to the variations of the crack length and energy release rate. The ultrasonic tester (Sitescan 240) with a straight beam probe of 10 mm in diameter and 4 MHz in

frequency was used and the glycerin was used as the couplant medium. The difference in sound pressure caused by variations in crack length on the adhesively bonded joint indicates the ratio of the 2nd reflection versus 1st reflection generated through the ultrasonic test.

3. ENERGY RELEASE RATE AND ULTRASONIC ATTENUATION COEFFICIENT

3.1. Compliance and Energy Release Rate

The energy release rate can be obtained by experimental measurement of compliances. When the static load, P, is subjected on an elastic body with the crack length, a, and thickness, B, if the crack propagates to a certain crack length, da, the compliance C and displacement δ, in the diagram of load-load point displacement are as follows:

$$C = \frac{\delta}{P} \tag{1}$$

In addition, the energy release rate, G and compliance, C, can be written as:

$$G = \frac{dU}{dA} = \frac{1}{B}\frac{dU}{da} = \frac{P^2}{2B}\frac{dC}{da} \tag{2}$$

where U refers to the elastic strain energy consumed during the propagation of a crack, and A is the size of an area where a crack has newly propagated.

3.2. Ultrasonic Attenuation Coefficient

The variation of sound pressure caused by ultrasonic attenuation when the ultrasonic wave passes through the couplant medium decreases in relation to the exponential functions.

In ASTM E.664-93, the apparent ultrasonic attenuation coefficient (α) without the effect of ultrasonic attenuation on the couplant medium can be represented as the following equation:

$$\alpha_0 = 20\frac{1}{2H}\log\frac{F_0}{F_n} \tag{3}$$

where F_0 refers to the initial sound pressure, F_n is the sound pressure when the reflection proceeds to the distance n, and H is the height of the specimen.

In an experiment, when ultrasonic wave is incident on the couplant medium, a layer of a certain thickness is formed between the probe and the specimen. The ultrasonic attenuation coefficient (α) which represents the ultrasonic attenuation caused by the couplant medium and that of the adhesive layer on the base material can be obtained as:

$$\alpha = \frac{1}{4H}\cdot\log\left[r_c^2\cdot r_m^2\cdot\left|\frac{F_n}{F_{n+1}-F_{n+2}} - \frac{F_{n+1}-F_{n+2}}{F_{n+2}-F_{n+3}}\right|\right] \tag{4}$$

where r_c is the reflection ratio of sound pressure in the couplant mediums, and r_m is the reflection coefficient of the sound pressure in the base material.

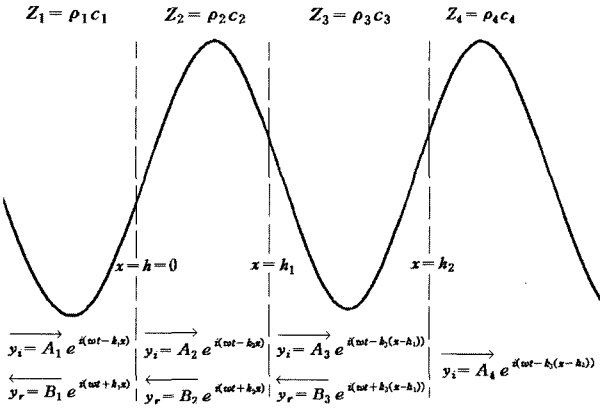

Figure 2. Diagram of incident and reflected ultrasonic waves on adhesive interfaces.

Equation (4) represents a linear ultrasonic wave and it is used to determine the ultrasonic attenuation coefficient in a homogeneous material. In this paper, we used equation (4).

3.3. Coefficients of Sound Pressure Reflection and Transmission

When the perpendicular ultrasonic wave passes through the couplant mediums, the reflection and transmission coefficients of the sound pressure should be taken into consideration owing to the acoustic impedance of each material. Thus, the equation to obtain a reflection coefficient of sound pressure when the ultrasonic wave is incident on two medium materials with different acoustic impedances, as shown in Figure 2, is as follows:

$$r_c = \frac{(Z_1/Z_2 - Z_2/Z_1)}{\sqrt{4\cot^2 kh + (Z_1/Z_2 + Z_2/Z_1)^2}}$$

$$r_m = \frac{(Z_2/Z_3 - Z_3/Z_2)}{\sqrt{4\cot^2 kh_1 + (Z_2/Z_3 + Z_3/Z_2)^2}} \tag{5}$$

where $k=2\pi/\lambda$, $\lambda=V/f$, λ is wavelength, V is the velocity of material, h and h_1 is the layer thickness of each couplant medium, respectively. Z_i is the acoustic impedance and f is the frequency of each material.

In Figure 2, when the base material, couplant medium and adhesive layer are considered, the transmission coefficient (t) is derived as the following equation:

$$t = \frac{2Z_1/Z_4}{B^* + C^* + D^* - E^*} \tag{6}$$

where,

$B^*=(Z_1/Z_4+1)\cos k_2 h_1\cdot\cos k_3(h_2-h_1)$

$C^*=i(Z_1/Z_2+Z_2/Z_4)\sin k_2 h_1\cdot\cos k_3(h_2-h_1)$

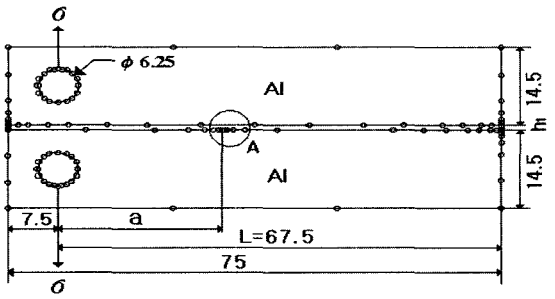

Figure 3. A typical mesh pattern of BEM model.

$$D^*=i(Z_1/Z_3+Z_3/Z_4)\cos k_2h_1\cdot\sin k_3(h_2-h_1)$$

$$E^*=(Z_1/Z_2\cdot Z_3/Z_4+Z_2/Z_3)\sin k_2h_1\cdot\sin k_3(h_2-h_1)$$

3.4. Analysis of the Boundary Element Method and Riplings Equation

Figure 3 illustrates a typical analysis model of the BEM for the specimen of adhesively bonded DCB joints as shown in Figure 1. The analysis model is half size of the real specimen shown in Figure 1. After obtaining the displacements for the load points according to the increasing crack lengths, the compliances can be calculated from the results of the BEM analysis. The BEM analysis consists of a 2-dimensional elastic program using Kelvin's fundamental solution. As for the meshes of model, the number of total nodes contained in the two regions of the adherends and one region of the adhesive layer is 326 nodes.

In order to verify the accuracy of the compliances calculated from the BEM analysis, they are compared with the results form the Ripling's equation. The Ripling's equation, as shown in equation (7), is an approximate equation to estimate the compliances of a DCB specimen prepared from a homogeneous material without an adhesive layer. However, it is also widely used in calculating the compliances of adhesively bonded DCB joints.

$$C = \frac{1}{3EI}[(a+a_0)^3 + H^2a] \tag{7}$$

where E is Young's modulus of the adherend, I is the moment of inertia, H is the height of the adherend, H^2a is the shear modification, and a is the crack length. a_0 is the rotation of the beam at crack-tip, and $a_0=0.6H$ in Ripling's equation.

4. RESULTS AND DISCUSSION

4.1. Compliance of Adhesively Bonded DCB Joints

Figure 4 shows the comparison of compliances obtained by Ripling's equation, the BEM analysis and the present experiment for the variation of the interfacial crack lengths.

The slight deviations in the values obtained from the experiment are considered to be the effects of the thickness of adhesive layer, the mechanical and physical properties of the materials, and the sound redundancy on each other. In addition, the differences between the BEM analysis and Ripling's equation indicate that the BEM analysis estimates more accurately an interface crack in adhesion conditions than that of Ripling's equation, as the latter is meant to be used for a homogeneous material.

4.2. Energy Release Rate of Adhesively Bonded DCB Joints

By substituting the compliances obtained from the experiment, the BEM analysis and Ripling's equation for an adhesively bonded DCB joint as shown in Figure 4, into equation (2), the energy release rates can be calculated.

Figure 5 compares the energy release rates obtained

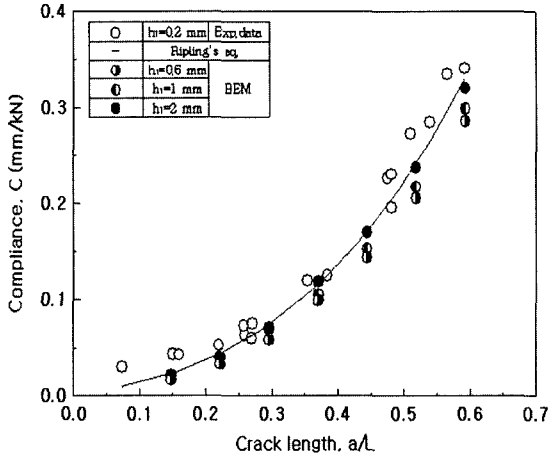

Figure 4. Relation between compliance and interfacial crack length.

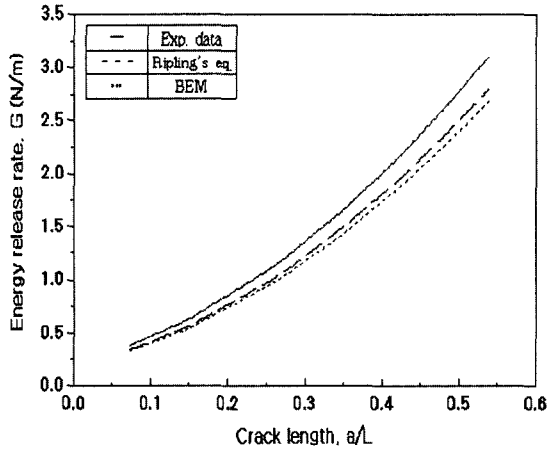

Figure 5. Relation between energy release rate and interfacial crack length.

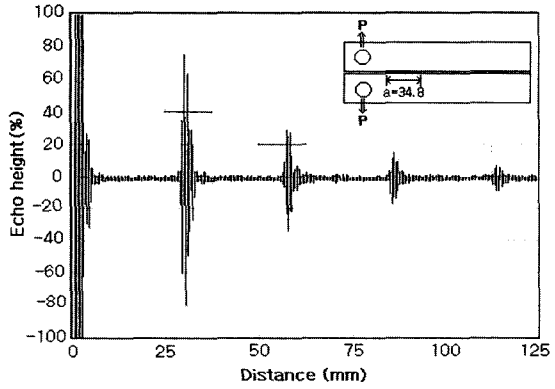

(a) Crack length, a=34.8 mm

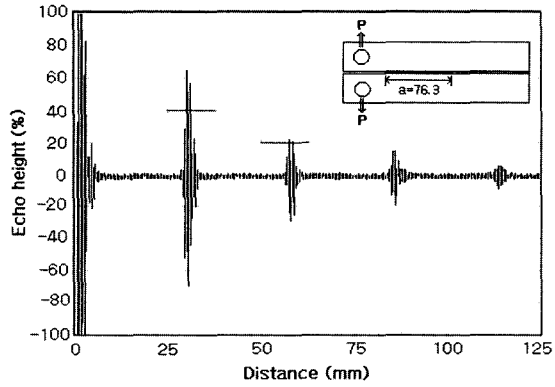

(b) Crack length, a=76.3 mm

Figure 6. Ultrasonic echo for an interface crack of adhesively bonded DCB joint.

from the results of the experiment, the BEM analysis and Ripling's equation. The energy release rate increases as the crack length increases and the rotation of the load point at the crack-tip increases with increasing crack length.

Figure 6 indicates the ultrasonic echo which occurs from an interface crack on an adhesively bonded DCB joint. As the interface crack propagates, the ultrasonic echo decreases owing to the conspicuous difference in sound pressure.

4.3. Interfacial Crack Length and Ratio of Ultrasonic Echo

Figure 7 demonstrates the relation between the compliance and the ratio of ultrasonic echo versus an interfacial crack length. As a crack propagates along the interface, the compliance increases and the ratio of ultrasonic echo decreases. In addition, while the interface crack propagates, the energy release rate increases in proportion to the interfacial crack length, and the ratio of ultrasonic echo decreases as shown in Figure 8. Therefore, the compliance and the energy release rate according to the interfacial crack length are in a relation of inverse proportion to the ratio of ultrasonic echo.

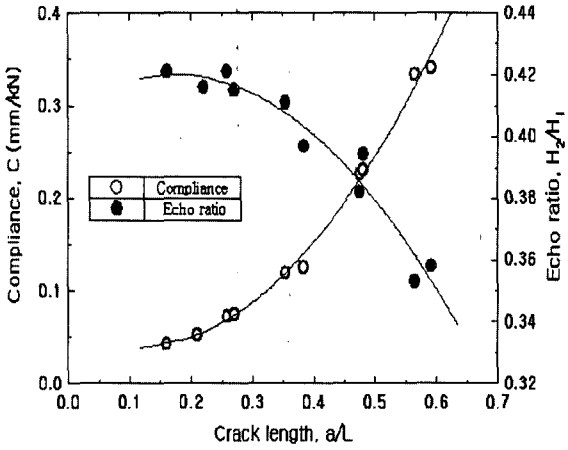

Figure 7. Relation between compliance and echo ratio versus interfacial crack length.

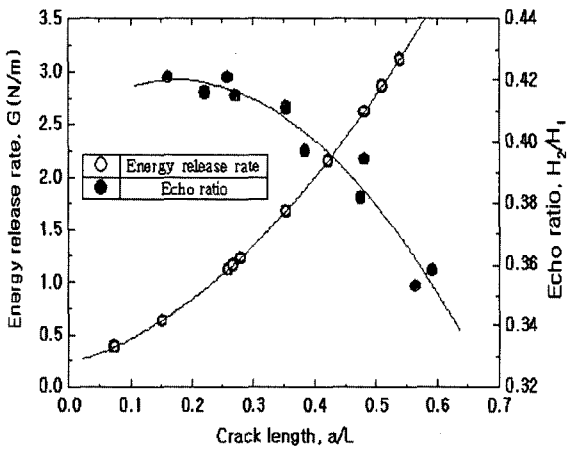

Figure 8. Relation between energy release rate and echo ratio versus interfacial crack length.

Figure 9 shows the correlations between the ultrasonic attenuation coefficient and the ratio of echo according to the interfacial crack length. As the ultrasonic attenuation coefficient increases, the ratio of ultrasonic echo decreases in inverse proportion to it.

4.4. Length of an Interfacial Crack and Ultrasonic Attenuation Coefficient

Figure 10 demonstrates the correlations between the ultrasonic attenuation coefficient and the energy release rate. As the ultrasonic attenuation coefficient increases, the energy release rate also increases in a straight line. The relationship between the energy release rate (G) and the ultrasonic attenuation coefficient (α) which were obtained through the present experiment, the BEM analysis and Ripling's equation can be described as follows:

$$G = 0.109\ \alpha - 5.972 \tag{8}$$

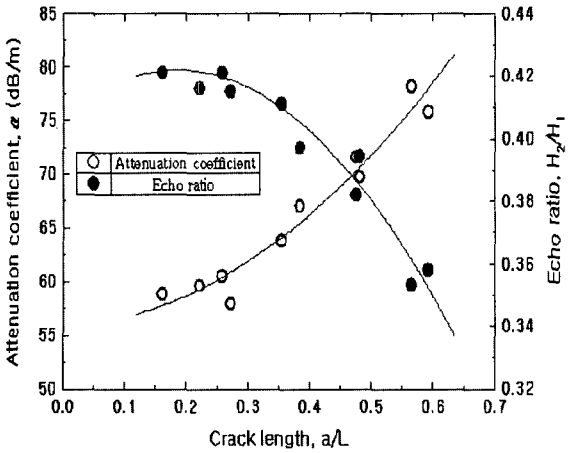

Figure 9. Relation between attenuation coefficient and echo ratio versus interfacial crack length.

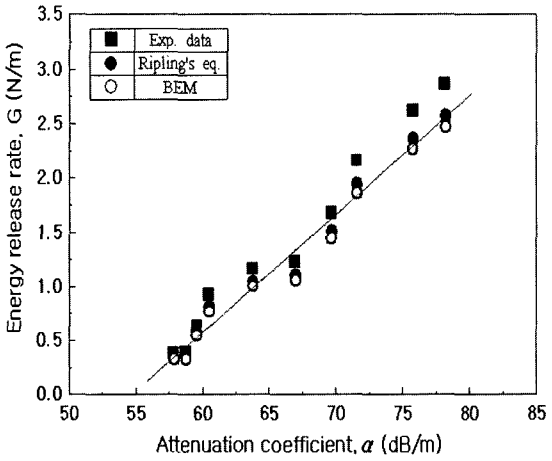

Figure 10. Relation between energy release rate and attenuation coefficient.

Figure 11 shows the relation between the ultrasonic attenuation coefficient and the interfacial crack length. As the ultrasonic attenuation coefficient increases, the interfacial crack length also increases proportionally. Increasing ultrasonic attenuation coefficient means that the ratio of ultrasonic echo decreases.

By using interfacial crack lengths, the energy release rates and the ultrasonic attenuation coefficients, the correlations between the interfacial crack length and the ultrasonic attenuation coefficient can be derived as the following equations.

$$\alpha = 58.872\left(\frac{a}{L}\right)^2 + 14.829\left(\frac{a}{L}\right) + 51.451 \quad (9)$$

Therefore, we can detect an interfacial crack length by using equations (8) and (9) after measuring the ultrasonic attenuation coefficient, and also recognize the correlations among the energy release rate, the ultrasonic attenuation coefficient and the interfacial crack length.

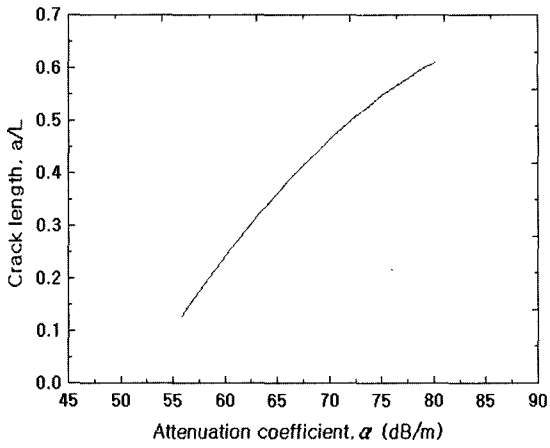

Figure 11. Relation between attenuation coefficient and interfacial crack length.

5. CONCLUSION

After comparing and considering the correlations between the interfacial crack length, ultrasonic attenuation coefficient and energy release rate obtained from the experiment on the adhesively bonded DCB joints, we came to the following conclusions :

(1) As the interfacial crack length increases, the ratio of ultrasonic echo decreases in inverse proportion.
(2) The energy release rate and an interfacial crack length are in proportional relations. Also, the energy release rate increases in a straight line as the ultrasonic attenuation coefficient increases.
(3) As the interfacial crack length increases, the ultrasonic attenuation coefficient increases in a slightly curved line, while the ratio of ultrasonic echo decreases.
(4) An interfacial crack length can be detected by measuring the ultrasonic attenuation coefficient and their correlations recognized.

ACKNOWLEDGMENT–This work was supported by the Soongsil University research fund.

REFERENCES

Biwa, S. and Watanabe, Y. (2003). Analysis of wave attenuation in unidirectional viscoelastic composites by a differential scheme. *Composite Science and Technology*, **63,** 237–247.

Castings, M. and Hosten, B. (2001). Lamb and SH waves generated and detected by air-coupled ultrasonic transducers in composite material plates. *NDT&E International*, **34,** 249–258.

Chung, N. Y., Park, S. I. and Lee, M. D. (2001). Detection of interface crack using ultrasonic method in adhesively bonded joint. *Transactions of the KSME* **25, 3,** 415–423.

Chung, N. Y., Park, S. I., Lee, M. D. and Park, C. H. (2002). Ultrasonic detection of interface crack in adhesively bonded DCB joints. *Int. J. Automotive Technology* **3,** 4, 157–163.

Derouiche, Z. and Dlebarre, C. (1996). Ultrasonic characterization of heterogeneous materials using a stochastic approach. *J. Acoust. Soc. Am.* **97, 4,** 2304–2315.

Jeong, H. D. and Shin, H. J. (1998). Detection of defects in a thin steel plate using ultrasonic guided wave. *J. KSNT* **18, 6,** 445–453.

Kishore, N. N. and Sridhar, I. (2000). Finite element modelling of the scattering of ultrasonic waves by isolated flaws. *NDT&E International,* **33,** 297–305.

Kline, R. A. (1983). Measurement of attenuation and dispersion using an ultrasonic spectroscopy technique. *J. Acoust. Soc. Am.* **76, 2,** 498–504.

Kline, R. A. and Hsiao, C. P. (1986). Nondestructive evaluation of adhesively bonded joint. *Journal of Engineering Materials and Technology,* **18,** 214–217.

Moriyama, S. and Kimura, K. (1998). Effect of surface roughness on sensitivity of ultrasonic normal beam testing. *J. JSNT* **47, 5,** 315–321.

Pecorari, C. (2000). Attenuation and dispersion of rayleigh waves propagation on a crack surface: An effective field approach. *Ultrasonic,* **38,** 754–760.

Ping, H. (2001). Acoustic dispersion and attenuation measurement using both transmitted and reflected pulses. *Ultrasonics,* **39,** 27–32.

Rippling, E. J., Mostovosy, S. and Patrick, R. L. (1964). Measuring fracture toughness of adhesive joints. *Materials Research Standard,* **14,** 129–134.

Si-Chaib, M. O., Djelouah, H. and Bocquet, M. (2000). Application of ultrasonic reflection mode conversion transducers in NDE. *NDT&E International,* **33,** 91–99.

Song, S. J., Choe, J. U. and Kim, H. J. (1998). A Study on elastic wave propagation for nondestructive evaluation of composite structures-An experimental approach. *Transaction of the KSME* **22, 6,** 978–989.

Xu, W. J. and Ourak, M. (1997). Angular measurement of acoustic reflection coefficient for substrate materials and layered structures by V(Z) technique. *NDT&E International,* **30,** 75–83.